Sensor applications

Energy-Efficient Data Transmission for Capacitive-Coupled Human Body Communication Systems

Luka Filipović[1], Marijan Herceg[1*], Jelena Vlaović[1], and Ertugrul Basar[2**]

[1]*Department of Communications, Faculty of Electrical Engineering, Computer Science and Information Technology, Osijek 31000, Croatia*

[2]*Department of Electrical and Electronics Engineering, Koc University, Istanbul 34450, Turkey*

[*]*Member, IEEE*

[**]*Senior Member, IEEE*

Manuscript received July 15, 2021; accepted September 18, 2021. Date of publication September 29, 2021; date of current version November 30, 2021.

Abstract—In this letter, an energy-efficient and low-complexity method for capacitive-coupled human body communication (CC-HBC) systems is proposed. In the proposed method, called impedance shift keying CC-HBC, the change of impedance between the transmitter's signal and the ground electrode is used to map information. In particular, the transmitter changes the condition of an electrical field generated by the receiver by changing the impedance between its signal and ground electrodes. Subsequently, by detecting the changes in the electric field, the receiver can demodulate the information sent by the transmitter. The CC-HBC channel is obtained using the transfer function method, while the performance of the proposed scheme is compared with frequency shift keying and on-off keying modulations.

Index Terms—Sensor applications, bit error rate (BER), human body communication, impedance shift keying (ISK).

I. INTRODUCTION

Human body communication (HBC)-based systems use the human body as a communication medium in an efficient manner. The basic principle of HBC systems was first presented by Zimmerman in 1995 [1].

Generally, HBC-based systems can be divided into three groups that differ by type of coupling: galvanic-coupled HBC (GC-HBC) [2], capacitive-coupled HBC (CC-HBC) [3], and magnetically coupled HBC (MC-HBC) [4]. In GC-HBC, data transmission is done with two electrodes that feed a small ac to the human body. CC-HBC systems similar to the GC-HBC systems use two electrodes per sensor node to transmit and receive data. However, the main difference between these two types is that in the CC-HBC, electrodes called signal electrodes in the transmitter and the receiver are placed on the human body, while the other two electrodes, called ground electrodes, can float, or the transceiver ground plane can be used as a floating ground. Therefore, on the transmitter side, in order to transmit the data, an alternate voltage source is fed to the signal electrode, which causes an alternate electrical flux in the proximity of the transmitter. In MC-HBC, the magnetic flux in the human body is provided by using an inductive loop, while on the receiver side, the transmitted data are demodulated after detecting the changes in the injected magnetic flux. Some of the commonly used modulation schemes in CC-HBC-based devices are ON–OFF keying (OOK) [5]–[7], frequency shift keying (FSK) [8], [9], and orthogonal frequency division multiplexing (OFDM) [10]. However, the aforementioned transmitters consists of different hardware components like oscillators, modulators, power amplifiers, FFT/IFFT, etc., which significantly increases overall hardware complexity and, thus, the power consumption.

Motivated by the aforementioned issues, in this letter, we propose a new and efficient modulation scheme for CC-HBC, called impedance shift keying CC-HBC (ISK-CC-HBC). In the ISK-CC-HBC system, information is mapped to the impedance between the transmitter's signal and ground electrodes. In particular, on the receiver side, the alternate voltage source is fed to the signal electrode through a shunt resistor, which produces an alternating electric field in the proximity of the receiver. Furthermore, by changing the impedance between the transmitter's signal and ground electrodes, changes in the electric field can be detected on the shunt resistor, and consequently, the information can be demodulated. Similar concept has been used in the inductively coupled systems by short circuiting the secondary *LC* tank [11]. However, in this letter, as far as we know, the concept of ISK is implemented for the first time in the capacitive coupled HBC systems.

Corresponding author: Luka Filipović (e-mail: luka.filipovic@ferit.hr).

Associate Editor: M. Kraft.

Digital Object Identifier 10.1109/LSENS.2021.3116354

II. ISK-CC-HBC SYSTEM MODEL

The block diagram of the proposed ISK-CC-HBC system is illustrated in Fig. 1. As shown, the transmitter and the receiver are placed on a human arm, and their signal electrodes are coupled through the human arm, while ground electrodes are capacitively coupled through the air. The developed electric circuit is modeled as in [3]. Generally, the communication channel consists of two parts: intrinsic and extrinsic. The intrinsic part includes human body tissues from the transmitter–human body interface to the human body–receiver interface. It is modeled as a parallel $R_{\text{body}} - C_{\text{body}}$ junction. R_{body} and C_{body} are varying parameters whose values depend on electrical features of the human body and distance between the transmitter and the receiver. The extrinsic part of the channel forms an electrode–skin interface, ground electrodes coupling of return path, and leakage capacitance caused by the capacitive coupling between the human body and the earth ground. Electrode–skin interfaces of signal electrodes from the transmitter (T_{x} SE) and the receiver (R_{x} SE) are modeled as a parallel $R_{\text{es}} - C_{\text{es}}$ junction. Moreover, there are paths caused by the signal leakage from the human body to an earth ground plane that are modeled as capacitance C_{leak} and capacitance between signal

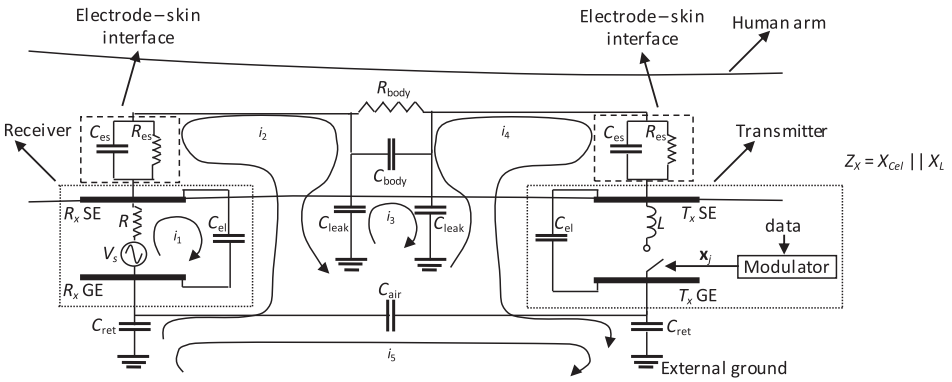

Fig. 1. ISK-CC-HBC communication system.

and ground electrodes C_{el}. C_{air} and C_{ret} denote coupling between the transmitter and the receiver ground electrodes (T_x GE and R_x GE) and coupling between ground electrodes and the earth ground plane, respectively. The extrinsic part of the channel changes with the distance between T_x GE and R_x GE and the earth ground.

In particular, C_{air} and C_{ret} for a square shape electrode can be calculated as [12]

$$C_{air} = \left[1 + 1.3105\left(\frac{D_{TR}}{l}\right)^{0.1075}\right]\frac{\varepsilon_0\varepsilon_r S}{D_{TR}} \tag{1}$$

$$C_{ret} = 2\left[1 + 3.1124\left(\frac{2D_{gnd}}{l}\right)^{0.9691}\right]\frac{\varepsilon_0\varepsilon_r S}{2D_{gnd}} \tag{2}$$

where ε_r and ε_0 are relative permittivity of the dielectric and the vacuum, respectively. S is a ground electrode surface, while l represents length of the one side of the square electrode. D_{TR} is a distance between the transmitter and the receiver, while D_{gnd} represents distance between the T_x GE and R_x GE and the earth ground. D_{gnd} and GND_{earth} values differ because of electrode thickness and distance between signal electrode and ground electrode. Furthermore, capacitance C_{leak}, for a human that is standing, can be calculated as [13]

$$C_{leak} = C_\infty + C_p \tag{3}$$

where C_∞ is the capacitance of the object placed noticeably above the earth ground, and C_p represents additional capacitance, which is the consequence of the vicinity effect of the earth ground. In this letter, it is assumed that the transmitter and the receiver are placed on human arm, which can be modeled as cylinder with diameter d and height h [13]. Subsequently, $C_{\infty,arm}$ and $C_{P,arm}$ can be calculated as

$$C_{\infty,arm} = 2\pi\varepsilon_0\frac{2d+h}{3} \tag{4}$$

$$C_{P,arm} = \pi\varepsilon_0 d\left[\frac{d}{4GND_{earth}} + \ln\left(1 + \frac{h}{GND_{earth}}\right)\right] \tag{5}$$

where GND_{earth} represents the distance between the arm and the earth ground, when the arm is in the horizontal position. Since both C_{ret} and C_{leak} depend on the distance to the ground D_{gnd}, the influence on the optimal inductance L is shown.

With assumption that observed part of the body is isotropic with equipotential cross sections, expressions for R_{body} and C_{body} can be calculated as in [14] with the following two equations:

$$R_{body} = \frac{a}{\sigma A} \tag{6}$$

$$C_{body} = \frac{\varepsilon_r\varepsilon_0 A}{a}. \tag{7}$$

Here, a and A are the observed body segment length and cross-sectional area. The mean value for the relative permittivity and conductivity for human arm is taken from [15] and [16].

As mentioned in [3] and [17], the electrode–skin interface can be modeled as a parallel $R_{es} - C_{es}$ junction. R_{es} models epidermis conductance, and C_{es} presents plate capacitor with tissues below epidermis and T_x SE/R_x SE as a capacitor plates, where epidermis is an insulator.

In particular, on the receiver side, a voltage V_s is fed to the signal electrode through the shunt resistor R. Subsequently, an electric field is applied near the receiver. On the transmitter side, data bits are fed to the modulator. According to the transmitted bit, i.e., 0 or 1, the switch is opened or closed. If the switch is closed, signal and ground electrodes are connected through the inductor L, and *vice versa*. Therefore, by closing and opening the switch, channel conditions change, i.e., the overall impedance between receiver's signal and ground electrodes changes, which causes the resistor R current i_R to change. Impedance Z_x, which causes the overall impedance change, will be equal to the parallel junction of C_{el} and L impedances (X_{Cel} and X_L) if binary "'1" is sent, or to the X_{Cel} otherwise. It should be emphasized that inductance was empirically chosen as the switching element and the influence of different switching elements on the system performance will be analyzed in our future work. Consequently, the change of the current i_R will cause the change of shunt voltage V_R of the resistor R.

Therefore, the bits on the transmitter side are modulated in the position of the switch $\mathbf{x}_j = [0\, I_j]^T$, where $j = 1, 2$, I_j is 1 in the jth position, and $(\cdot)^T$ is transpose operator. It is worth noting that a similar concept called space shift keying is widely used in radio frequency communications [18]. The signal at the receiver can be expressed as

$$e = \sqrt{\psi_b}\mathbf{a}\mathbf{x}_j + n \tag{8}$$

where ψ_b represents the average signal-to-noise ratio per bit, while the vector $\mathbf{a} = [a_1\, a_2]$ presents two different HBC channels caused by switch position on the transmitter side. n is an additive white Gaussian noise (AWGN) with a complex Gaussian distribution, with zero mean and unit variance. The vector of proper channel conditions $\mathbf{a}$ can be obtained using the transfer function V_R/V_S in a similar way as in [13] and [19].

On the receiver side, the voltage V_R, detected on the shunt resistor R, is used to demodulate the received signal. As mentioned earlier, the transmitter changes the amplitude and phase of the current i_r, by including inductance L to the circuit if binary "'1" is sent or by removing it from the circuit if binary "0" is sent. In order to demodulate the received signal, it is necessary to estimate the channel condition,

i.e., the V_R/V_S ratio of the corresponding data symbol transmission. A maximum likelihood (ML) detector is used for equally likely activated HBC channels. The ML detector estimates the index $\hat{j}$ of the corresponding channel as [18]. We therefore have (9), shown at the bottom of the page, and

$$V_R = i_1 R. \tag{10}$$

$$\hat{j} = \arg\min_m |e - \sqrt{\psi_b} a_m|^2, \quad m \in \{1, 2\}. \tag{11}$$

According to [18], the bit error probability (BEP) probability of ISK-CC-HBC is given as

$$P_{b,\mathrm{ISK}} = Q\left(\sqrt{\frac{\psi_b}{2}|a_1 - a_2|^2}\right) \tag{12}$$

where $Q(\cdot)$ is the tail probability of the standard Gaussian distribution. As seen from (5), the selection of a_1 and a_2 is very important to minimize the BEP, which will be discussed in the next section.

III. PERFORMANCE EVALUATION

In this section, the performance evaluation of the proposed ISK-CC-HBC is presented. In order to present a realistic situation, CC-HBC channel parameters are selected as follows. The transmitter and the receiver are placed on the forearm, while the chosen distance between them is 10 cm. The distance between the signal electrode and the ground electrode on both i.e., the transmitter and the receiver, is 1 cm. The dimensions of all four electrodes are 2 × 2 cm. The average distance between the human arm and the earth ground is about 1 m, and therefore, this value was used. Furthermore, from [3], [12], and [20], other CC-HBC parameters are selected. CC-HBC parameters used in the simulations are $C_{\mathrm{ret}} = 959.62$ fF, $C_{\mathrm{el}} = 354.16$ fF, $C_{\mathrm{air}} = 90.595$ fF, $C_{\mathrm{leak}} = 3.6046$ pF, $C_{\mathrm{es}} = 5.5$ pF, $R_{\mathrm{es}} = 250\ \Omega$, $R_{\mathrm{body}} = 157.19\ \Omega$, and $C_{\mathrm{body}} = 56.3267$ pF. The frequency of the sinusoidal signal with V_S voltage is 21 MHz, according to the IEEE 802.15.6 standard [21], while the resistance R value is set to $50\,\Omega$. It should be emphasized that channel model can be applied on other body parts by recalculating/measuring channel parameters. All simulations are made in MATLAB software using a channel model from [3], while the simulation parameters are given as follows.

Optimal inductance value for each $\mathrm{GND_{earth}}$ is determined with the maximum normalized Euclidean distance. Namely, when inductance L is active, impedance Z_{x} on the transmitter side will be changed. Consequently, V_R will be changed. Optimal inductances L for $\mathrm{GND_{earth}}$ values between 0.01 and 1.8 m are shown in Fig. 2. It can be seen that dependence is almost constant when $\mathrm{GND_{earth}}$ is above 0.5 m. Similarly, it can be seen in Fig. 2 for R_{body} values between 1 and 5000 Ω with $\mathrm{GND_{earth}}$ value fixed at 1 m. Consequently, the optimal L value will not change with hand position changes when the person is standing, walking, or doing some motions during these actions.

The described scenario considers two realizations of the CC-HBC channel. In particular, the constellation point $a_2 = 0.0310 + 0.9995i$ represents channel conditions when the inductance L is inactive, while

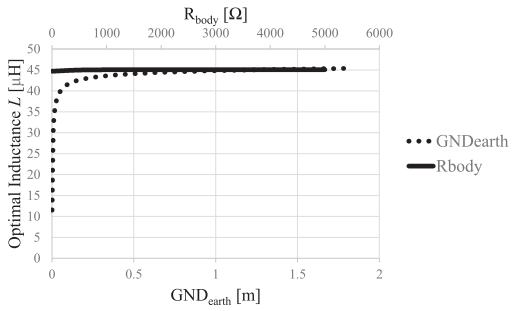

Fig. 2. Optimal inductance L for different $\mathrm{GND_{earth}}$ and R_{body} values.

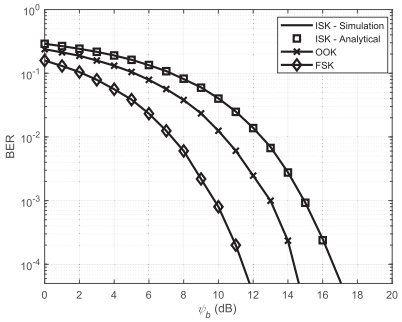

Fig. 3. BER comparison of OOK, FSK, and ISK-CC-HBC.

the constellation point a_1 represents channel conditions when the inductance L is active. In order to obtain the optimal inductance L value, its influence on the normalized Euclidean distance between a_1 and a_2 is analyzed, and it is found that the Euclidean distance between a_1 and a_2 is maximized for $L = 45\ \mu$H. For $L = 45\ \mu$H, the constellation point a_1 is equal to $0.7416 + 0.6708i$.

In Fig. 3, the bit error rate (BER) performance comparison of ISK-CC-HBC, FSK, and OOK is shown. As seen from Fig. 3, as expected, OOK and FSK outperform ISK-CC-HBC for all ψ_b. However, this decrease in the BER performance is compensated by the reduced hardware complexity. It should be also noticed that there is a perfect match between analytical and simulation results.

However, in order to show the advantages of the proposed system, the comparison with the OOK and FSK modulation regarding the hardware complexity is performed. In particular, from Table 1, it can be seen that ISK-CC-HBC modulation outperforms OOK and FSK in hardware complexity. It arises from the fact that in order to transmit its data, ISK-CC-HBC only uses a switch and an inductor in order to change the channel condition between the transmitter and the receiver. Therefore, it should be emphasized that there is no need for an oscillator and power amplifier on the transmitter side in the ISK-CC-HBC scheme, due to the fact that the transmitter data are sent by changing the electric field, which is generated by the receiver.

$$\begin{bmatrix} V_S \\ 0 \\ 0 \\ 0 \\ 0 \end{bmatrix} = \begin{bmatrix} R + Z_{\mathrm{el}} & -Z_{\mathrm{el}} & 0 & 0 & 0 \\ -Z_{\mathrm{el}} & Z_{\mathrm{el}} + Z_{\mathrm{es}} + Z_{\mathrm{leak}} + Z_{\mathrm{ret}} & -Z_{\mathrm{leak}} & 0 & -Z_{\mathrm{ret}} \\ 0 & -Z_{\mathrm{leak}} & 2Z_{\mathrm{leak}} + Z_{\mathrm{body}} & Z_{\mathrm{leak}} & 0 \\ 0 & 0 & -Z_{\mathrm{leak}} & Z_{\mathrm{leak}} + Z_{\mathrm{es}} + Z_{\mathrm{x}} + Z_{\mathrm{ret}} & -Z_{\mathrm{ret}} \\ 0 & -Z_{\mathrm{ret}} & 0 & -Z_{\mathrm{ret}} & 2Z_{\mathrm{ret}} + Z_{\mathrm{air}} \end{bmatrix} \times \begin{bmatrix} i_1 \\ i_2 \\ i_3 \\ i_4 \\ i_5 \end{bmatrix}, \tag{9}$$

Table 1. Comparison of Different Schemes

First author, reference	*Modulation*	*Hardware complexity*
Cho, [5]	OOK	Wien-bridge oscillator, 2 modulators, driver
Zhao, [6]	OOK	oscillator, mixer, power amplifier
Shih, [8]	DPFSK	digital frequency interpolators, ring oscillators, multiplexer
Yile, [9]	FSK	oscillator, harmonics injection-locking, driver
This work	ISK	analog switch, inductor

IV. CONCLUSION

In this letter, a novel energy-efficient ISK-CC-HBC scheme is proposed. In particular, in the proposed scheme, the receiver generates an electric field in its proximity by applying ac voltage to its signal electrode. Furthermore, the transmitter changes the ambient electric field condition by connecting and disconnecting inductance between its signal and ground electrodes in order to map the information in an index modulation fashion. Moreover, it is shown that the BER performance of the ISK-CC-HBC scheme is higher compared to OOK and FSK. However, this BER performance degradation has been compensated by the extremely low hardware complexity of the ISK transmitter structure.

Due to the fact that sensor nodes in the wireless body area network are battery-powered devices placed on the human body, where low hardware complexity, small dimensions, and ultralow power consumption are the key requirements, the proposed method is an attractive solution for CC-HBC systems.

ACKNOWLEDGMENT

This work was supported in part by the Faculty of Electrical Engineering, Computer Science and Information Technology Osijek projects "IZIP2019". The work of Ertugrul Basar was supported in part by the Scientific and Technological Research Council of Turkey (TUBITAK) under Grant 218E035.

REFERENCES

[1] T. G. Zimmerman, "Personal area networks(PAN): Near-field intra-body communication," Master's thesis, Mass. Inst. Technol., Cambridge, MA, USA, 1995.

[2] M. A. Callejon, J. Reina-Tosina, D. Naranjo-Hernández, and L. M. Roa, "Galvanic coupling transmission in intrabody communication: A finite element approach," *IEEE Trans. Biomed. Eng.*, vol. 61, no. 3, pp 775–783, Mar. 2014.

[3] M. D. Pereira, G. A. Alvarez-Botero, and F. R. de Sousa, "Characterization and modeling of the capacitive HBC channel," *IEEE Trans. Instrum. Meas.*, vol. 64, no. 10, pp 2626–2635, Oct. 2015.

[4] J. Park and P. P. Mercier, "Magnetic human body communication," in *Proc. 37th Annu. Int. Conf. IEEE Eng. Med. Biol. Soc.*, Milan, Italy, 2015, pp 1841–1844.

[5] H. Cho *et al.*, "79 pJ/b 80 mb/s full-duplex transceiver and a 42.5 uW 100 kb/s super-regenerative transceiver for body channel communication," *IEEE J. Solid-State Circuits*, vol. 51, no. 1, pp 310–317, Jan. 2016.

[6] J. Zhao *et al.*, "A 4-Mbps 41-pJ/bit on-off keying transceiver for body-channel communication with enhanced auto loss compensation technique," in *Proc. IEEE Asian Solid-State Circuits Conf.*, Macao, China, Nov. 2019, pp. 173–176.

[7] B. Chatterjee, A. Srivastava, D.-H. Seo, D. Yang, and S. Sen, "A context-aware reconfigurable transmitter with 2.24 pJ/bit, 802.15.6 NB-HBC and 4.93 pJ/bit, 400.9 MHz MedRadio modes with 33.6 % transmit efficiency," in *Proc. IEEE Radio Freq. Integr. Circuits Symp.*, Los Angeles, CA, USA, Aug. 2020, pp. 75–78.

[8] H. Y. Shih, Y. C. Chang, C. W. Yang, and C. C. Chen, "A low-power and small chip-area multi-rate human body communication DPFSK transceiver for wearable devices," *IEEE Trans. Circuits Syst., II, Exp. Briefs*, vol. 67, no. 7, pp 1234–1238, Jul. 2020.

[9] L. Yile, G. W. Ling, and V. V. Kulkarni, "A 29 pJ/bit FSK transmitter for WBAN applications," in *Proc. IEEE Int. Conf. Electron Devices Solid-State Circuits*, Singapore, Jun. 2015, pp. 182–185.

[10] W. Saadeh, M. A. B. Altaf, H. Alsuradi, and J. Yoo, "A 1.1-mW ground effect-resilient body-coupled communication transceiver with pseudo OFDM for head and body area network," *IEEE J. Solid-State Circuits*, vol. 52, no. 10, pp 2690–2702, Oct. 2017.

[11] S. Mandal and R. Sarpeshkar, "Power-efficient impedance-modulation wireless data links for biomedical implants," *IEEE Trans. Biomed. Circuits Syst.*, vol. 2, no. 4, pp 301–315, Dec. 2008.

[12] J. Mao, H. Yang, and B. Zhao, "An investigation on ground electrodes of capacitive coupling human body communication," *IEEE Trans. Biomed. Circuits Syst.*, vol. 11, no. 4, pp 910–919, Aug. 2017.

[13] K. Zhang, Q. Hao, Y. Song, J. Wang, R. Huang, and Y. Liu, "Modeling and characterization of the implant intra-body communication based on capacitive coupling using a transfer function method," *Sensors*, vol. 14, pp 1740–1756, Jan. 2014.

[14] N. Cho, J. Yoo, S.-J. Song, J. Lee, S. Jeon, and H. J. Yoo, "The human body characteristics as a signal transmission medium for intrabody communication," *IEEE Trans. Microw. Theory Techn.*, vol. 55, no. 5, pp 1080–1086, May 2007.

[15] S. Gabriel, R. W. Lau, and C. Gabriel, "The dielectric properties of biological tissues: III. Parametric models for the dielectric spectrum of tissues," *Phys. Med. Biol.*, vol. 41, pp 2271–2293, Nov. 1996.

[16] S. Huclova, D. Erni, and J. Fröhlich, "Modelling and validation of dielectric properties of human skin in the MHz region focusing on skin layer morphology and material composition," *J. Phys. D, Appl. Phys.*, vol. 45, no. 2, Jan. 2012, Art. no. 025301.

[17] G. S. Anderson and C. G. Sodini, "Body coupled communication: The channel and implantable sensors," in *Proc. IEEE Int. Conf. Body Sensor Netw.*, Cambridge, MA, USA, May 2013, pp. 1–5.

[18] J. Jeganathan, A. Ghrayeb, L. Szczecinski, and A. Ceron, "Space shift keying modulation for MIMO channels," *IEEE Trans. Wireless Commun.*, vol. 8, no. 7, pp 3692–3703, Jul. 2009.

[19] M. Herceg, L. Filipović, T. Matić, and G. Kaddoum, "Inductance index modulation for human body communication systems," *IEEE Wireless Commun. Lett.*, vol. 8, no. 3, pp 937–940, Jun. 2019.

[20] R. Xu, H. Zhu, and J. Yuan, "Electric-field intrabody communication channel modeling with finite-element method," *IEEE Trans. Biomed. Eng.*, vol. 58, no. 3, pp 705–712, Mar. 2011.

[21] *IEEE Standard for Local and Metropolitan Area Networks–Part 15.6: Wireless Body Area Networks*, IEEE Std. 802.15.6-2012, pp 1–271, Feb. 2012.